Response to Increasing Southern Hemisphere Winds in CCSM4

Article *in* Journal of Climate · October 2011

DOI: 10.1175/JCLI-D-10-05011.1

2 authors, including:

Peter Gent
National Center for Atmospheric Research
110 PUBLICATIONS **9,315** CITATIONS

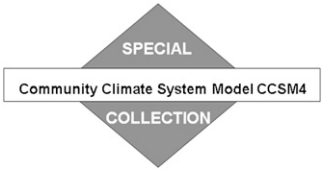

Response to Increasing Southern Hemisphere Winds in CCSM4

PETER R. GENT AND GOKHAN DANABASOGLU

National Center for Atmospheric Research, Boulder, Colorado*

(Manuscript received 10 December 2010, in final form 5 April 2011)

ABSTRACT

Results from two perturbation experiments using the Community Climate System Model version 4 where the Southern Hemisphere zonal wind stress is increased are described. It is shown that the ocean response is in accord with experiments using much-higher-resolution ocean models that do not use an eddy parameterization. The key to obtaining an appropriate response in the coarse-resolution climate model is to specify a variable coefficient in the Gent and McWilliams eddy parameterization, rather than a constant value. This result contrasts with several recent papers that have suggested that coarse-resolution climate models cannot obtain an appropriate response.

1. Introduction

Several recent papers have questioned whether the coarse-resolution ocean components used in climate models can simulate an appropriate response to increasing Southern Hemisphere winds: Hallberg and Gnanadesikan (2006), Hogg et al. (2008), Boning et al. (2008), Screen et al. (2009), and Spence et al. (2010). This subject has arisen because the response to increasing Southern Hemisphere winds in ocean models with either eddy-permitting or eddy-resolving resolution, and using no eddy parameterization has been described in several recent papers discussed below.

Hallberg and Gnanadesikan (2006) use an isopycnal coordinate model, Meredith and Hogg (2006) and Hogg et al. (2008) use a three-layer quasigeostrophic model, Screen et al. (2009) use the Ocean Circulation and Climate Advanced Model, Spence et al. (2010) use the University of Victoria (U-Vic) climate model, and Farneti et al. (2010) use the Geophysical Fluid Dynamics Laboratory (GFDL) CM2.4 climate model. All these papers document the result that when the Southern Hemisphere winds increase, the northward surface Ekman flow and, therefore, the mean flow meridional overturning circulation (MOC) increase in the region of the Antarctic Circumpolar Current (ACC). This MOC is the streamfunction calculated from the zonally integrated time-mean flow. In addition, they all show that the level of eddy activity increases, resulting in more southward eddy heat transport across the ACC. Some papers say that the ACC is in an ''eddy saturated state,'' defined as when the stronger mean flow MOC due to the increased winds is balanced by the stronger MOC due to increased eddy activity, defined as deviations from the time mean. It is difficult to determine from some of these papers the extent to which the two components balance, because they do not show the MOC and concentrate instead on the eddy heat transport. Farneti et al. (2010) force the ocean very strongly with a zonal wind stress perturbation that nearly doubles the maximum value and moves it somewhat to the south. They show with the eddy-permitting resolution of the CM2.4 that the eddy MOC cancels a very large fraction of the stronger mean flow MOC, but the cancellation is not exact. It is difficult to know what the correct response should be, because results vary across these different simulations described above, none of which use an eddy-resolving ocean component in a full climate model. However, it is very clear that the eddy response to increasing winds must oppose the mean flow MOC and heat transport, and balance a large fraction of the increase in these mean quantities.

If the effect of increased eddy activity is to be parameterized in coarse-resolution ocean models, then the

* The National Center for Atmospheric Research is sponsored by the National Science Foundation.

Corresponding author address: Peter R. Gent, NCAR, P.O. Box 3000, Boulder, CO 80307.
E-mail: gent@ucar.edu

DOI: 10.1175/JCLI-D-10-05011.1

Gent and McWilliams (1990) (GM) coefficient, κ, also needs to increase. In all the papers referenced above that use GM, except Farneti et al. (2010), κ was specified as a constant. It is now clear that if this is done, then the coarse-resolution model will get the wrong response, because eddy effects near the ACC cannot increase with the wind forcing. We are not the first to reach this conclusion, because Fyfe et al. (2007) chose to increase κ in proportion to the increasing zonal-mean wind stress, which is prescribed in the simple atmosphere component of the U-Vic climate model. Thus, κ increased from the standard value of 800 $m^2 s^{-1}$ in 1850 to 1100 $m^2 s^{-1}$ in 2100 at the end of their twenty-first century projection run. They do not show any MOCs but show increased southward eddy heat transport across the ACC that leads to a 25% increase in warming south of 52°S compared to a run where κ was kept constant. However, the many prescriptions to specify a variable κ such as Visbeck et al. (1997), except the one used in Fyfe et al. (2007), only use ocean variables and not the wind stress. We think it is much preferable to use ocean variables to specify κ, and not ocean forcing quantities, because eddy activity is much more strongly correlated to steep density slopes and baroclinic instability than to the wind stress.

An example of a variable κ specification is the GFDL climate model CM2.1, where it is proportional to the average of the horizontal density gradient over the depth range 100 m–2 km and is constant in the vertical. Farneti et al. (2010) show that in CM2.1 the eddy MOC due to the perturbation that doubles the Southern Hemisphere zonal wind stress does not increase to match the increase in the mean flow MOC. The reason is that the CM2.1 κ is capped at 600 $m^2 s^{-1}$, which is an appropriate value for the ACC with present day winds but is not nearly large enough when the wind stress is doubled. Farneti and Gent (2011) show results when the cap is doubled to 1200 $m^2 s^{-1}$ and the density slope where κ is clipped is increased from $1/500$ to $1/100$. Then the eddy response to the wind stress perturbation is much larger and balances well over half of the increase in the mean flow MOC. The cancellation is not quite as large as in the CM2.4 model, which has eddy-permitting ocean resolution and no GM closure. However, Farneti and Gent (2011) show that if κ has a good variable definition with weak restrictions, then the CM2.1 climate model can respond appropriately to the large perturbation in Southern Hemisphere wind stress.

Very recent independent work by Hofmann and Morales-Maqueda (2011) has also shown an appropriate response to increasing Southern Hemisphere winds in an ocean-alone study. Here, the GM coefficient is specified by the Visbeck et al. (1997) scheme using a vertically averaged Richardson number and a mixing length scale, and is constant in the vertical.

In this article, we show results using the recently completed Community Climate System Model version 4 (CCSM4). Two perturbation experiments are run where the Southern Hemisphere zonal wind stress is increased, first by 50% south of 35°S and second by the same large perturbation used in Farneti et al. (2010). This explores the response to increasing Southern Hemisphere winds in a different climate model, where the GM κ is specified differently from that in CM2.1, in order to determine whether the Farneti and Gent (2011) and Hofmann and Morales-Maqueda (2011) results are robust across different climate models.

2. Description of the CCSM4

The CCSM4 is a state-of-the-art climate model with a standard resolution of near 1° in all components and is documented in Gent et al. (2011). The ocean component uses a latitude/longitude grid in the Southern Hemisphere and has 60 vertical levels with 10-m levels in the upper 200 m. It uses the GM parameterization, which is implemented as follows near the ocean surface: In the mixed layer the eddy-induced velocity is horizontal with no vertical shear, and diffusion is in the horizontal direction. Between the mixed layer and the deeper ocean where GM is applied, there is a transition layer across which the mixed layer and deeper forms are matched. This implementation, and the resulting improved solutions, is documented in Danabasoglu et al. (2008). The coefficient κ is prescribed as a function of space and time, following the implementation described in Danabasoglu and Marshall (2007). At the base of the transition layer, κ is set to the reference value of 3000 $m^2 s^{-1}$ but then decreases in the vertical following the square of the local buoyancy frequency. This vertical decay mimics the vertical distribution of eddy kinetic energy in the ocean. The vertical average of κ is much closer to the familiar values of several hundred often used when κ is specified as a constant. In this formulation there is no need for slope clipping in the upper ocean, although a slope cutoff is applied to the isopycnal diffusion and GM terms in the deeper ocean. The ocean component is described in Danabasoglu et al. (2011).

Two perturbation experiments have been run for 100 yr, starting from year 863 of the 1850 preindustrial control run described in Gent et al. (2011). In the first (PERT1), the zonal wind stress forcing the ocean component is multiplied by the factor 1.5 south of 35°S, with this factor linearly reducing to 1 between 35° and 25°S. This increases the maximum zonally averaged zonal wind stress from 0.19 to 0.28 N m^{-2} but does not change the latitude of the maximum wind stress (see Fig. 1). In

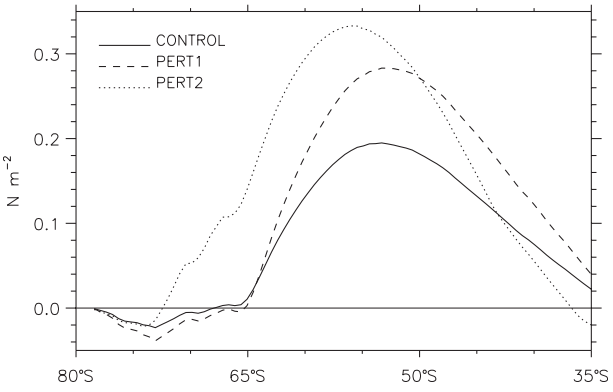

FIG. 1. The zonally averaged zonal wind stress (N m^{-2}) south of 35°S from the control, PERT1, and PERT2 runs.

the second experiment (PERT2), the large pertubation zonal wind stress used in the GFDL CM2.1 model in Farneti et al. (2010) and Farneti and Gent (2011) is added in the CCSM4. This increases the maximum zonally averaged wind stress to 0.33 N m^{-2} and also moves the location of the maximum about 3° to the south (see Fig. 1). As is usual in this type of perturbation experiment, the increased zonal wind is not used to calculate the atmosphere-to-ocean heat and freshwater fluxes, and the increased zonal stress is not felt directly by the atmosphere component. However, there is an indirect effect on the coupled system through changes to the sea surface temperature.

3. Perturbation experiment results

All results shown in this section are averages over 20 yr: 943–962 of the control run and 81–100 of the two perturbation runs. Figure 2a shows the GM κ averaged over the upper kilometer in the control run, assuming that κ is the reference value above the base of the transition layer. The largest values over 1500 m^2 s^{-1} occur in shallow water near the continents and topographic features such as the Campbell Plateau. In the open ocean, large values occur in a zonal band on the northern flank of the ACC. Smaller values of $<$600 m^2 s^{-1} occur in a band between the ACC and Antarctica to the south. Figure 2b shows the difference between the κ values over the upper kilometer in the PERT1 and control runs. It shows that κ increases over most of the Southern Hemisphere south of 35°S. Increases of up to 400 m^2 s^{-1} occur at the latitudes where the zonal wind stress increase is largest. These increases in κ are a result of much deeper mixed layers and stratification changes, which are the realistic consequences of the much stronger winds. A deeper mixed layer results in a larger eddy effect over a greater depth, and then larger κ values throughout the water column.

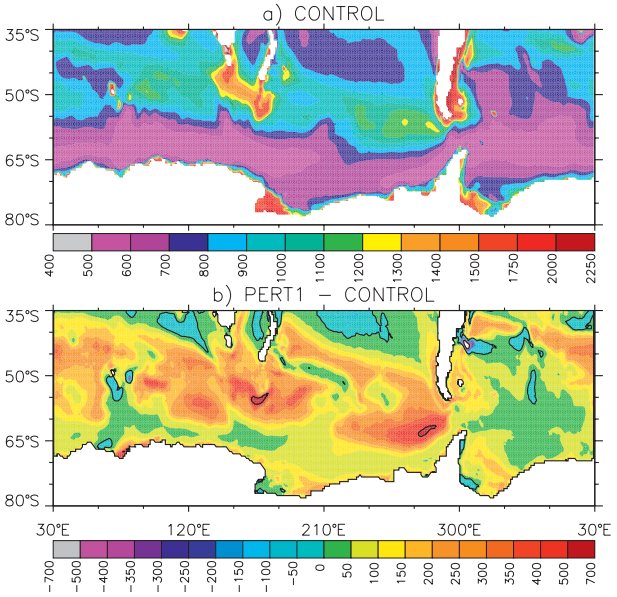

FIG. 2. The GM coefficient κ (m^2 s^{-1}) averaged over the upper kilometer, south of 35°S: (a) control and (b) PERT1 minus control.

Figure 3 shows the Southern Hemisphere MOC from the control and PERT1 runs plotted against potential density referenced to 2-km depth (σ_2). It shows the MOCs from the mean flow, the GM eddy flow, and their total, which is often called the residual circulation. The mean and GM MOC maxima include the ACC region between 50° and 60°S at σ_2 values between 36.2 and 37.2. The maximum in the mean flow MOC increases from 16.7 Sv (1 Sv $\equiv 10^6$ m^3 s^{-1}) in the control run to 20.2 Sv in PERT1 because of the 50% increase in the zonal wind stress. The negative GM MOC increases from 12.8 to 15.5 Sv in the same location, so that the total MOC maximum only increases by 1.4 Sv. The figure shows that the parameterized GM MOC, representing an increased level of eddy activity, balances a large fraction of the mean flow MOC increase, which is consistent with results using either eddy-permitting or eddy-resolving ocean models without GM. The PERT2 run MOC results are broadly similar; although the fraction of the mean flow MOC increase balanced by GM is reduced a little but is still over ½. This reduced balancing by GM is probably caused by the latitude of the maximum zonal wind stress moving 3° to the south in this run. The PERT2 MOC results using the CCSM4 are very comparable to those using the CM2.1 with the κ cap of 1200 m^2 s^{-1}, shown in Fig. 7 of Farneti and Gent (2011).

Figure 4 shows the potential density referenced to the surface (σ_0) south of 35°S over the upper 1.5 km from the control and perturbation runs. Figure 4a shows that there are only small, subtle changes in isopycnal slopes in PERT1, with a little steepening in the upper ocean

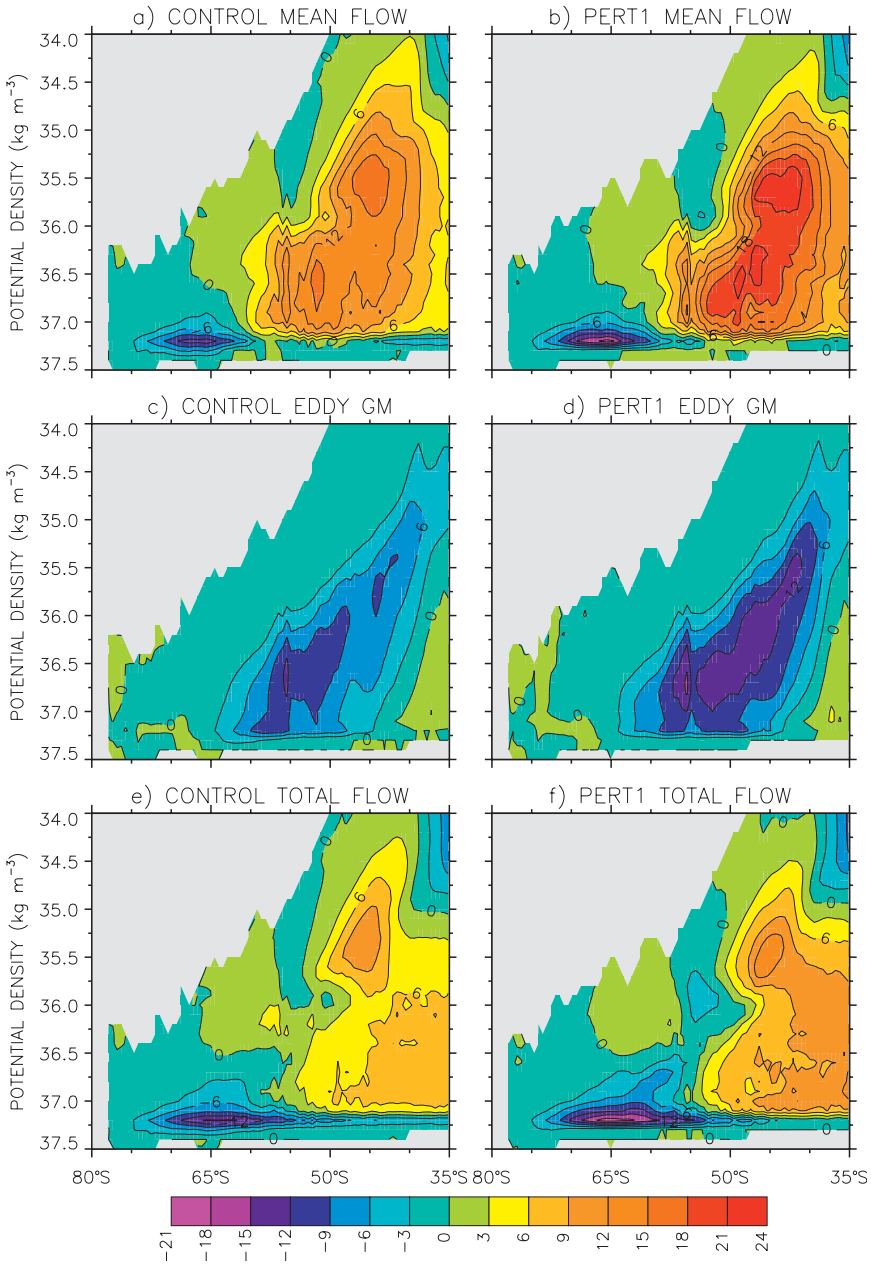

FIG. 3. The MOC (Sv) south of 35°S against potential density referenced to 2 km, σ_2: Mean flow from (a) control and (b) PERT1; eddy GM from (c) control and (d) PERT1; and total flow from (e) control and (f) PERT1. Positive and negative contours indicate clockwise and anticlockwise circulations.

above 500 m. This is very consistent with the eddy GM MOC balancing most, but not all, of the increase in the mean flow MOC. Figure 4b shows that in the PERT2 run there are also some subtle changes in isopycnal slopes, but the main change is a deepening of the isopycnals by up to 100 m. This figure can be compared to Fig. 7 in Farneti et al. (2010), which shows the results of imposing the same wind stress perturbation in the CM2.1 with the small κ cap of 600 m^2 s^{-1} and CM2.4. The CCSM4 isopycnal changes are much smaller than the quite large changes seen in CM2.1 and are closer to the results from CM2.4, which has eddy-permitting ocean resolution and no GM. The PERT2 wind stress changes are very much larger than the wind stress change observed over the last 30 yr. If this smaller observed wind stress change, which is like PERT2 but with a much smaller amplitude, was

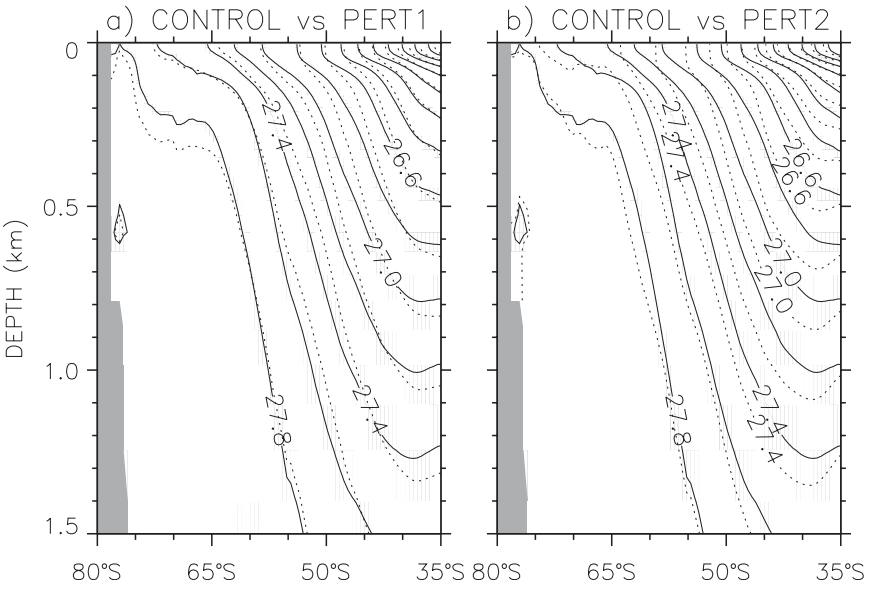

FIG. 4. Potential density referenced to the surface σ_0 (kg m^{-3}) south of 35°S over the upper 1.5 km: (a) control (solid) and PERT1 (dotted); and (b) control (solid) and PERT2 (dotted). The contour interval is 0.2 kg m^{-3}.

put into the CCSM4, then the isopycnals would deepen a little with very small changes in their slopes. This is what has been observed during this time period over the upper 2 km (see Boning et al. 2008, their Fig. 4a). The Drake Passage transport in PERT1 only increases by 7 Sv compared to the control run value of 176 Sv. In contrast, the PERT2 Drake Passage transport increases by 75 Sv compared to the control run, which is mostly the result of the maximum zonal wind stress moving 3° to the south.

Figure 5 shows the northward heat transport by the mean flow, the eddy GM, and the total south of 35°S from the control and two perturbation runs. The total includes the transport by the isopycnal diffusion term, which is always to the south at these latitudes, and is almost the same in all three runs. Figure 5 shows that the larger northward mean flow transport between 40° and 50°S in PERT1 is mostly balanced by the larger southward GM eddy transport. The southward total transport in PERT1 is increased a little in the ACC region between 50° and 60°S, which is largely due to an increase in the GM eddy transport. These changes are consistent with the mean and eddy MOCs shown in Fig. 3. Figure 5 shows larger changes in PERT2 because the transport maxima are moved to the south by the more southerly location of the maximum zonal wind. However, again the changes in mean flow heat transport are largely compensated by the increased GM eddy southward heat transport between 43° and 53°S. South of 60°S, both the mean and GM eddy southward transports increase, so that the total transport in PERT2 is significantly larger than in the control run. The larger southward eddy heat transport in both perturbation experiments is consistent with results from eddy-resolving and eddy-permitting models in Hallberg and Gnanadesikan (2006), Fyfe et al. (2007), Hogg et al. (2008), and Screen et al. (2009).

Figure 6 shows the zonally averaged potential temperature differences between the perturbation and control runs south of 35°S down to 1.5 km. The PERT1 run in Fig. 6a produces small temperature changes in the ACC region, but a larger change of >1°C is located farther

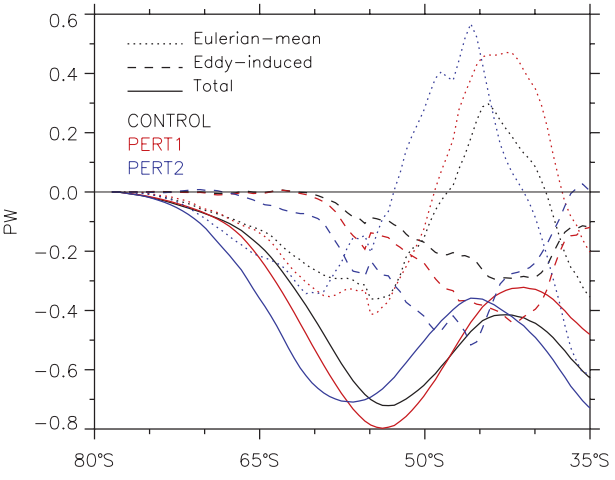

FIG. 5. Northward heat transport (PW) by the mean flow, eddy GM, and the total flow south of 35°S for control (black), PERT1 (red), and PERT2 (blue).

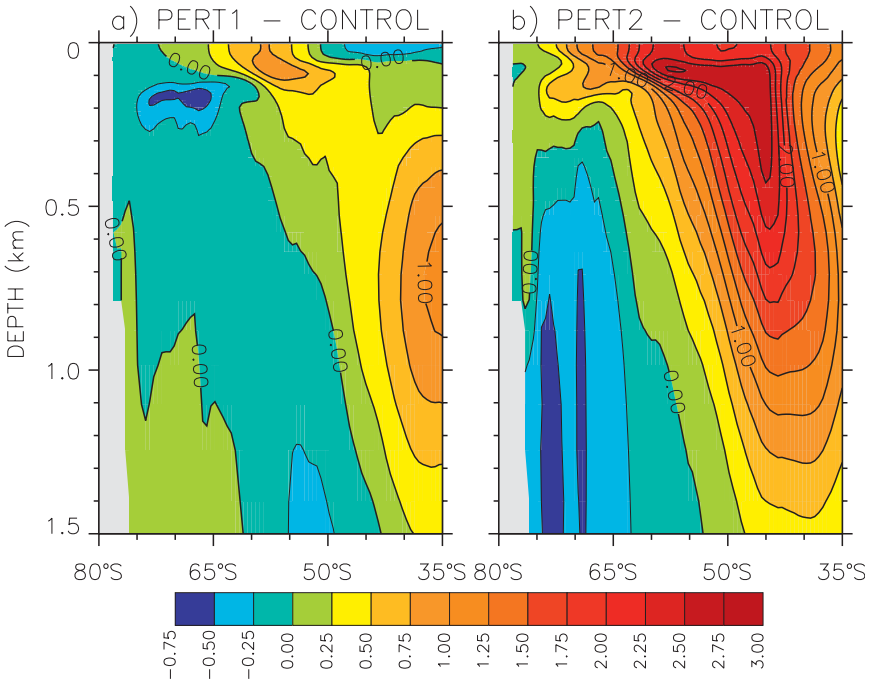

FIG. 6. Zonally averaged potential temperature (°C) south of 35°S over the upper 1.5 km: (a) PERT1 minus control and (b) PERT2 minus control.

north in the midlatitude gyre. In contrast, Fig. 6b shows quite large changes to the upper ocean in PERT2, with warming of >2°C reaching from the surface to below 500 m between 40° and 50°S. This results from the strong temperature gradients in the upper ocean moving south in response to the southward shift in the maximum zonal winds. Figure 6b shows warming down to 1 km between 35° and 60°S, so that the warming of the Southern Ocean over the recent past is more likely because of the southward shift in the maximum winds, rather than because of their increased strength (see also Fyfe 2006).

4. Conclusions

The conclusion from this article is that, if variable κ is specified as in CCSM4, then this climate model can get an appropriate response to increasing Southern Hemisphere winds. However, if κ is a constant, as was the case in CCSM3, then the climate model will get an incorrect response. This supports the conclusions in Hofmann and Morales-Maqueda (2011) and Farneti and Gent (2011), where κ has different variable definitions in the horizontal and is constant in the vertical. When κ is allowed to vary depending on prognostic model fields, then it can naturally respond to deeper mixed layers and changes in the isopycnal slopes caused by changes in the wind stress forcing. The different choices for variable κ in Hofmann and Morales-Maqueda (2011), Farneti and Gent (2011), and CCSM4 all seem to work satisfactorily, but there is still much work ongoing into how to specify variable κ.

REFERENCES

Boning, C. W., A. Dispert, M. Visbeck, S. R. Rintoul, and F. U. Schwarzkopf, 2008: The response of the Antarctic Circumpolar Current to recent climate change. *Nat. Geosci.,* **1,** 864–869.

Danabasoglu, G., and J. Marshall, 2007: Effects of vertical variations of thickness diffusivity in an ocean general circulation model. *Ocean Modell.,* **18,** 122–141.

——, R. Ferrari, and J. C. McWilliams, 2008: Sensitivity of an ocean general circulation model to a parameterization of near-surface eddy fluxes. *J. Climate,* **21,** 1192–1208.

——, S. Bates, B. Briegleb, M. Jochum, S. Jayne, W. Large, S. Peacock, and S. Yeager, 2011: The CCSM4 ocean component. *J. Climate,* in press.

Farneti, R., and P. R. Gent, 2011: The effects of the eddy-induced advection coefficient in a coarse-resolution coupled climate model. *Ocean Modell.,* **39,** 135–145, doi:10.1016/j.ocemod.2011.02.005.

——, T. L. Delworth, A. J. Rosati, S. M. Griffies, and F. Zeng, 2010: The role of mesoscale eddies in the rectification of the Southern Ocean response to climate change. *J. Phys. Oceanogr.,* **40,** 1539–1557.

Fyfe, J. C., 2006: Southern Ocean warming due to human influence. *Geophys. Res. Lett.,* **33,** L19701, doi:10.1029/2006GL027247.

——, O. A. Saenko, K. Zickfeld, M. Eby, and A. J. Weaver, 2007: The role of poleward-intensifying winds on Southern Ocean warming. *J. Climate,* **20,** 5391–5400.

Gent, P. R., and J. C. McWilliams, 1990: Isopycnal mixing in ocean circulation models. *J. Phys. Oceanogr.,* **20,** 150–155.

——, and Coauthors, 2011: The Community Climate System Model version 4. *J. Climate,* **24,** 4973–4991.

Hallberg, R., and A. Gnanadesikan, 2006: The role of eddies in determining the structure and response of the wind-driven Southern Hemisphere overturning: Results from the Modeling Eddies in the Southern Ocean (MESO) project. *J. Phys. Oceanogr.,* **36,** 2232–2252.

Hofmann, M., and M. A. Morales-Maqueda, 2011: The response of Southern Ocean eddies to increased midlatitude westerlies: A non-eddy resolving model study. *Geophys. Res. Lett.,* **38,** L03605, doi:10.1029/2010GL045972.

Hogg, A. M., M. P. Meredith, J. R. Blundell, and C. Wilson, 2008: Eddy heat flux in the Southern Ocean: Response to variable wind forcing. *J. Climate,* **21,** 608–620.

Meredith, M. P., and A. M. Hogg, 2006: Circumpolar response of Southern Ocean eddy activity to a change in the southern annular mode. *Geophys. Res. Lett.,* **33,** L16608, doi:10.1029/2006GL026499.

Screen, J. A., N. P. Gillett, D. P. Stevens, G. J. Marshall, and H. K. Roscoe, 2009: The role of eddies in the Southern Ocean temperature response to the southern annular mode. *J. Climate,* **22,** 806–818.

Spence, P., J. C. Fyfe, A. Montenegro, and A. J. Weaver, 2010: Southern Ocean response to strengthening winds in an eddy-permitting global climate model. *J. Climate,* **23,** 5332–5343.

Visbeck, M., J. Marshall, T. Haine, and M. Spall, 1997: Specification of eddy transfer coefficients in coarse-resolution ocean circulation models. *J. Phys. Oceanogr.,* **27,** 381–402.